

## RESEARCH ARTICLE

# Epithelioid Glioblastomas and Anaplastic Epithelioid Pleomorphic Xanthoastrocytomas—Same Entity or First Cousins?

Sanda Alexandrescu<sup>1</sup>; Andrey Korshunov<sup>2,3</sup>; Siang Hui Lai<sup>4</sup>; Salma Dabiri<sup>5</sup>; Sushama Patil<sup>6</sup>; Rong Li<sup>7</sup>; Chie-Schin Shih<sup>8</sup>; Jose M. Bonnin<sup>9</sup>; Jonathan A. Baker<sup>10</sup>; Emma Du<sup>11</sup>; David W. Scharnhorst<sup>12</sup>; David Samuel<sup>13</sup>; David W. Ellison<sup>14</sup>; Arie Perry<sup>1</sup>

<sup>1</sup> Department of Pathology, University of California, San Francisco, CA.

<sup>2</sup> Clinical Cooperation Unit Neuropathology, German Cancer Research Center (DKFZ), Heidelberg, Germany.

<sup>3</sup> Department of Neuropathology, Heidelberg University Hospital, Heidelberg, Germany.

<sup>4</sup> Department of Pathology, Singapore General Hospital, Singapore.

<sup>5</sup> Department of Pathology, Good Samaritan Hospital, San Jose, CA.

<sup>6</sup> Department of Pathology, Apollo Specialty Hospital, Chennai, India.

<sup>7</sup> Department of Pathology, Children's Hospital of Alabama, Birmingham, AL.

<sup>8</sup> Department of Pediatrics,

<sup>9</sup> Department of Pathology, Indiana University, Indianapolis, IN.

<sup>10</sup> Department of Pathology, Texas Health Presbyterian Hospital, Dallas, TX.

<sup>11</sup> Department of Pathology, Scripps Clinic, La Jolla, CA.

<sup>12</sup> Department of Pathology,

<sup>13</sup> Department of Pediatric Oncology, Children's Hospital Central California, Madera, CA.

<sup>14</sup> Department of Pathology, St. Jude Children's Research Hospital, Memphis, TN.

## Keywords

*BRAF<sup>V600E</sup>*, epithelioid, glioblastoma, *ODZ3*, pediatric, pleomorphic, prognosis, xanthoastrocytoma.

## Corresponding author:

Sanda Alexandrescu, MD, Department of Pathology, University of California, San Francisco, 505 Parnassus Ave. MSB 580, San Francisco, CA 94143 (E-mail: [sanda.alexandrescu@ucsf.edu](mailto:sanda.alexandrescu@ucsf.edu))

Received 8 June 2015

Accepted 27 July 2015

Published Online Article Accepted 3 August 2015

doi:10.1111/bpa.12295

## Abstract

Epithelioid glioblastoma (eGBM) and pleomorphic xanthoastrocytoma (PXA) with anaplastically transformed foci (ePXA) show overlapping features. Eleven eGBMs and 5 ePXAs were reviewed and studied immunohistochemically. Fluorescence *in situ* hybridization for *EGFR* amplification, *PTEN* deletion and *ODZ3* deletion was also performed, with Illumina 450 methylome analysis obtained in five cases. The average age for eGBM was 30.9 (range 2–79) years, including five pediatric cases and a M : F ratio of 4.5. The ePXA patients had a M : F ratio of 4 and averaged 21.2 (range 10–38) years in age, including two pediatric cases. Six eGBMs and two ePXAs recurred (median recurrence interval of 12 and 3.3 months, respectively). All tumors were composed of solid sheets of loosely cohesive, “melanoma-like” cells with only limited infiltration. ePXAs showed lower grade foci with classic features of PXA. Both tumor types showed focal expression of epithelial and glial markers, retained INI1 and BRG1 expression, occasional CD34 positivity, and lack of mutant IDH1 (R132H) immunoreactivity. *BRAF V600E* mutation was present in four eGBMs and four ePXAs. *ODZ3* deletion was detected in seven eGBMs and two ePXAs. *EGFR* amplification was absent. Methylome analysis showed that one ePXA and one eGBM clustered with PXAs, one eGBM clustered with low-grade gliomas, and two eGBMs clustered with pediatric-type glioblastomas. Common histologic, immunohistochemical, molecular and clinical features found in eGBM and ePXA suggest that they are closely related or the same entity. If the latter is true, the nomenclature and WHO grading remains to be resolved.

## INTRODUCTION

Glioblastoma (GBM), WHO grade IV, is one of the most malignant cancer types in adult and pediatric populations. Part of its original name of “multiforme” reflects its remarkable histologic variability, with the World Health Organization (WHO) recognizing several subtypes as either clinically and molecularly distinct variants or

merely morphologic patterns with no obvious differences from classic GBM (14).

Epithelioid glioblastoma (eGBM) is one of the rarest variants and is not yet recognized as a subtype in the 2007 WHO classification scheme (14). It is characterized by relatively solid aggregates of large “melanoma-like” epithelioid cells with abundant eosinophilic cytoplasm, some eccentrically placed nuclei,

prominent nucleoli and distinct cellular membranes (8, 22, 23). While one study makes a distinction between eGBM and rhabdoid GBM based on the focal loss of INI1 immunoreactivity in rhabdoid areas (9), there is considerable overlap and others use these terms interchangeably (11, 17, 27). The diagnosis of eGBM is often challenging and only a few small series have been reported in the adult and pediatric populations (2, 8, 19). Excluding other CNS tumors with epithelioid features is critical and it has been noted that a subset of anaplastic pleomorphic xanthoastrocytomas (PXAs) have similar pathologic features (7, 14) and even some overlapping molecular findings (5, 8). In our practice, we have occasionally encountered PXAs with anaplastic transformation showing cytologic characteristics that are indistinguishable from those of eGBM. In a similar fashion, a case report of eGBM arising in a PXA has recently been reported (26). As with eGBM, PXAs with anaplastic transformation most often afflict children and young adults, although cases in older patients have also been reported (3, 15).

A recent case report of an eGBM with *BRAF*<sup>V600E</sup> mutation used comparative genomic hybridization (CGH) to identify three copy number alterations located in different morphologic areas; there were three alterations restricted to the epithelioid areas: a homozygous deletion in intron 3 of *LSAMP* at 3q13, a hemizygous deletion of *ODZ3* at 4q34.3–4q35.1 and a hemizygous deletion in *LRP1B* on chromosome 2 (19). *ODZ3* gene was reported as a potent tumor suppressor gene, which has also been implicated in the pathogenesis of lung adenocarcinoma, adrenal carcinoma and neuroblastoma (13, 16, 18). In this study, we analyzed the available clinical, histopathologic and molecular data of 16 eGBMs and PXAs with epithelioid forms of anaplastic transformation (ePXA), with the intent of establishing if these tumors share a common tumorigenic background. To explore this possibility further, we performed fluorescence *in situ* hybridization for *ODZ3* deletion and methylome signature studies in subsets of both ePXA and eGBM.

## MATERIALS AND METHODS

### Case selection

As defined previously by Kleinschmidt-DeMasters *et al*, eGBM had to be composed in great part (more than 30%–40% of the tumor) of patternless sheets of loosely cohesive, epithelioid or melanoma-like cells with distinct cellular borders, abundant eosinophilic cytoplasm, and central or slightly eccentric nuclei with distinct nucleoli (8). Anaplastic features such as high mitotic index, microvascular proliferation and necrosis are variably superimposed and some evidence of glial differentiation was required. ePXA was similarly defined as a glioma that is composed predominantly (more than 30%–40% of the tumor) of epithelioid cells with the same features as seen in eGBM, but also demonstrates at least a small area of classic PXA.

With Institutional Review Board approval, we searched the archives of the Department of Pathology at UCSF Medical Center and found 12 cases that fit the histologic criteria for eGBM or ePXA within the January 2013 to April 2015 interval. With the exception of one ePXA, the rest of the cases were consults submitted to one of the authors (AP). None of these 12 cases have been previously reported. In addition, four eGBMs were provided

by the Institute of Pathology, Ruprecht-Karls University, Heidelberg, Germany, and were also part of a separate previously reported study of pediatric GBMs (10). For the purpose of this study, patients 18 years old or younger were considered pediatric.

### Clinical and radiographic information

All available clinical and neuroimaging studies (images and/or radiology reports) were reviewed from electronic patient records and submitted consult materials.

### Histology

Histological review and immunohistochemical studies were performed on 4  $\mu$  sections of formalin-fixed paraffin-embedded tissue. Immunohistochemical assessment was performed using antibodies against: glial fibrillary acidic protein (GFAP) (DAKO 1:300, Carpinteria, CA), Olig2 (Immuno Bio Labs 1:200, Minneapolis, MN), neurofilament (NF) protein (Cell Marque predilute, Rocklin, CA), synaptophysin (Cell Marque 1:100, Rocklin, CA), CD34 (Leica Biosystems predilute, Buffalo Grove, IL), EMA (Leica Biosystems predilute, Buffalo Grove, IL), vimentin (Leica Biosystems predilute, Buffalo Grove, IL), Ki67 (Leica Biosystems predilute, Buffalo Grove, IL), NeuN (Chemicon International 1:4000, Dublin, OH), MAP2 (Sigma-Aldrich 1:20 000, St. Louis, MO), p53 (Vector Laboratories, 1:100, Burlingame, CA), IDH1(R132H) (Dianova 1:500, Hamburg, Germany), *BRAF*<sup>V600E</sup> (Spring Bioscience 1:50, Pleasanton, CA) and INI1 (SMARCB1 gene product) (Becton Dickinson 1:100, San Jose, CA). An antibody against BRG1 (SMARCA4 gene product) (Abcam 1:100, Cambridge, MA) was applied to three ePXA and four eGBM cases in the histology laboratory at St. Jude's Children's Research Hospital. H3.3 K27M (Millipore 1:500, Billerica, CA) immunohistochemical stain was performed on eight of the eGBM cases. The presence or absence of tumoral staining, the general extents of expression (eg, diffuse, patchy, focal, rare) and staining localization patterns were noted. The p53 immunostain was reported as positive when greater than 10% p53 nuclear positivity was present (25). The immunohistochemical studies were limited in one case of eGBM and a case of ePXA because of insufficient material. Digital photomicrographs were taken using an Olympus DP72 camera.

### Fluorescence *in situ* hybridization

To investigate the deletion status of the *ODZ3* gene, we utilized a commercial *ODZ3* gene bacterial artificial clone (BAC) (RP11-713021; 4q34.3–4q35.1) and confirmed a portion of its published sequence using polymerase chain reaction (PCR).

This probe was directly labeled with rhodamine and paired with a SpectrumGreen labeled CEP 4 commercial FISH probe (06J37-014, Abbott Molecular) using previously reported methodology (20).

Green and red signals were enumerated under an Olympus BX 41 fluorescence microscope. Cases with more than 25% cells demonstrating a ratio of 1 red : 2 green signals were considered deleted. For control specimens, we performed FISH for *ODZ3* gene deletion on slides from 10 epilepsy resections (five focal cortical dysplasia and five mesio-temporal sclerosis).

The EGFR amplification and PTEN deletion FISH assays were designed and performed in the Molecular Laboratory in the Department of Pathology at UCSF Medical Center using the Vysis™ dual-color DNA probe set. EGFR amplification was diagnosed when the ratio of EGFR to CEP7 exceeded 2.2. PTEN (10q) deletion was identified when the ratio of PTEN to CEP10 is less than 0.8 and the percent of cells with <2 signals is greater than 20%. Monosomy 10 required that the percentage of cells with <2 CEP10 signals exceeded 30%.

### Genome-wide methylation studies

Genome-wide methylation patterns were studied in four pediatric cases of eGBM and an adult case of ePXA in the Department of Pathology at Heidelberg University Hospital in Germany, utilizing the method previously reported by Korshunov *et al* (10). Briefly, the DNA was extracted from tumors and analyzed for genome-wide methylation patterns using the Illumina Human Methylation450 BeadChip (450k) array. Custom approaches described by Sturm *et al* (24) were utilized to process the DNA methylation data and the detection of copy number aberrations. The most variably methylated probes across the dataset were used for unsupervised hierarchical clustering, and samples were clustered using 1-Pearson correlation coefficient as the distance measure and average linkage. Methylation probes were reordered by hierarchical clustering using Euclidean distance and average linkage.

## RESULTS

### Clinical data

A summary of clinical findings is found in Table 1. There were 13 male (81.3%) (nine eGBMs, four ePXAs) and 3 female (18.8%) (two eGBMs and one ePXA) patients. Seven of the cases (43.8%) (two ePXAs and five eGBMs) were pediatric and nine (56.2%) (three ePXAs and six eGBMs) were adult. The

average ages for ePXA and eGBM patients were 21.2 (range 10–38) and 30.9 (range 2–79) years, respectively. All ePXAs arose in the cerebral hemispheres (one frontal, one fronto-temporal, two occipital, one temporal). Two of the eGBMs arose in the thoracic spine and nine in the cerebral hemispheres (six temporal, one frontal, one parietal and one adjacent to the lateral ventricle).

The neuroradiology reports and/or images were reviewed in six eGBM and all ePXA cases. The tumors showed nonspecific features overall, but regardless of diagnosis, most commonly featured well demarcated, contrast enhancing, superficial cerebral masses. The associated edema was more pronounced in the eGBM cases (Figure 1). Three of the ePXAs (60%) and two of the eGBMs (18.2%) had leptomeningeal spread at diagnosis.

The median follow-up interval for all patients was 8 months (range 2–65 months). Two ePXAs (40%) and six eGBMs (54.5%) recurred; the median interval to recurrence for the former was 3.3 months and for the latter was 12 months. Two patients with eGBM, one adult and one pediatric, died of disease 4 and 14 months after diagnosis, respectively. However, most of the patients remain alive at last follow-up with survival times already exceeding 2 years in three eGBM cases (33, 38 and 65 months at last follow-up), suggesting that long survival times are seen in a subset.

### Histopathology and molecular features

The histopathologic and immunohistochemical findings are summarized in Tables 2 and 3, while the molecular findings are summarized in Table 4. Epithelioid foci were defined by the presence of large “melanoma-like” tumor cells with abundant eosinophilic cytoplasm and nuclei that are occasionally eccentrically placed and suggestive of rhabdoid cytology (Figure 2). This was typically accompanied by loose cellular cohesion, a high mitotic index and foci of tumor necrosis, with microvascular proliferation seen in a subset. All ePXAs showed at least focal areas of classic PXA by

**Table 1.** Summary of the clinical information. Abbreviations: NA = not applicable; NK = not known; ePXA = epithelioid pleomorphic xanthoastrocytoma; eGBM = epithelioid glioblastoma; GTR = gross total resection; STR = subtotal resection.

Case No.	Age	Sex	Diagnosis	Location	Resection type	Recurrence/progression	Recurrence interval (months)	Follow-up (months)	Alive at last follow-up
1	38	M	ePXA	Left occipital	GTR	Yes	1.5	2	Yes
2	25	M	ePXA	Right frontal	GTR	No	NA	10	Yes
3	13	M	ePXA	Right occipital	GTR	Yes	5	7	Yes
4	20	F	ePXA	Right temporal	GTR	No	NA	13	Yes
5	10	M	ePXA	Right fronto-temporal	STR	No	NA	3	Yes
6	38	M	eGBM	T7–8	STR	No	NA	4	No
7	11	M	eGBM	Right temporo-parietal	GTR	Yes	53	65	Yes
8	21	F	eGBM	Right fronto-temporal	NK	NK	NK	0	NK
9	79	M	eGBM	Right temporal	NK	Yes	8	8	Yes
10	70	F	eGBM	Right temporal	NK	No	NA	5.2	Yes
11	12	M	eGBM	Frontal	STR	Yes	12	14	No
12	11	M	eGBM	Temporal	STR	Yes	24	38	Yes
13	2	M	eGBM	Lateral ventricle	GTR	No	NA	16	Yes
14	14	M	eGBM	Parietal	GTR	Yes	12	33	Yes
15	26	M	eGBM	T9–12	STR	No	NA	2	Yes
16	56	M	eGBM	Right temporal	NK	Yes	2	2	Yes

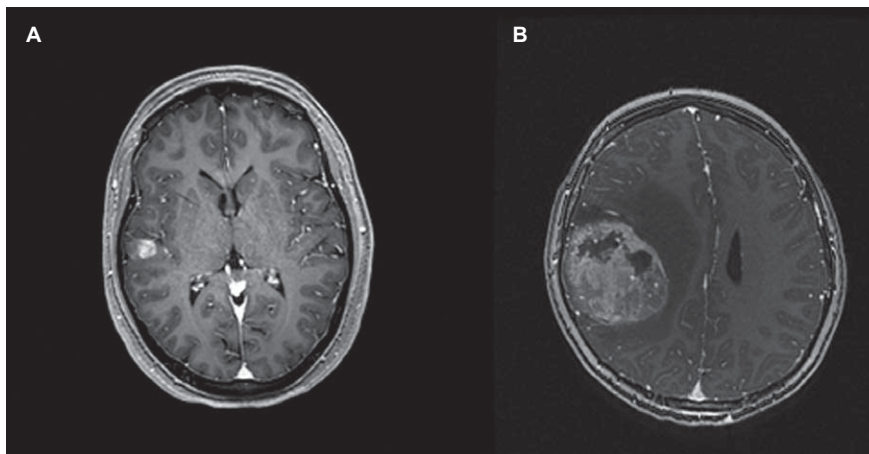


**Figure 1.** **A.** Post-gadolinium t1 axial magnetic resonance image demonstrating a well-defined enhancing superficial ePXA in the right temporal lobe, involving mostly the cortex; surrounding edema is not seen. **B.** Post-gadolinium magnetic resonance t1 axial image demonstrating a well-defined, heterogeneously enhancing superficial eGBM with marked surrounding edema.

definition (Figure 3A), including spindled cells variably forming fascicles, large bizarre mono- and multinucleated cells with or without lipidized cytoplasm, perivascular lymphocytic cuffing and eosinophilic granular bodies; these features were absent from eGBMs and from the epithelioid portions of ePXAs (Figure 3B). The eGBMs in our series were composed almost exclusively of epithelioid cells with the cytologic features described above, and only three of the cases demonstrated a definite infiltrative component, resembling a classic diffuse astrocytoma. Frequent mitoses (more than 5 per 10 high-power fields), areas of necrosis, including pseudopalisading, and microvascular proliferation were present in the epithelioid foci of all cases. The reticulin stain showed a rich intercellular meshwork in the classic PXA areas in three of the five cases, whereas the epithelioid areas were reticulin poor in all five. Classic PXA areas were extensively positive for GFAP (Figure 3C) and Olig2, whereas these glial markers highlighted only rare cells in epithelioid areas (Figure 3D). A NF immunostain demonstrated

occasional entrapped axons at the periphery of the ePXAs, but otherwise highlighted the mostly solid growth patterns; similarly, eGBMs displayed a mostly solid growth pattern with infiltration only at the periphery in seven (30%) of the cases and a more diffusely infiltrative growth pattern in three (30%) cases. There was patchy EMA positivity in all ePXAs and in eight of the eGBMs (72.7%). Four ePXAs (80%) and four eGBMs (40%) showed patchy synaptophysin positivity in tumor cells. Three of the ePXAs demonstrated scattered cells with membranous CD34 immunopositivity involving both classic PXA and epithelioid foci (60%) (Figure 3E,F), whereas occasional CD34-positive tumor cells were encountered in four eGBMs (40%). The vimentin immunostain was extensively positive in all cases tested. All cases had retained nuclear INI1 expression, with BRG1 expression similarly retained in all seven cases tested. All eGBMs were negative for IDH1 (R132H) mutant protein expression. A p53 immunostain was performed on 10 cases and it was positive in two ePXAs

**Table 2.** Histopathologic features of 5 ePXAs and 11 eGBMs. Abbreviations: ePXA = epithelioid pleomorphic xanthoastrocytoma; eGBM = epithelioid glioblastoma.

Case No.	Diagnosis	Mitotic rate (per 10 HPF)	Necrosis	Microvascular proliferation	Eosinophilic granular bodies
1	ePXA	6	Geographic, large foci	Present, one focus	Present
2	ePXA	20	Pseudopalisading and geographic	Present	Present; rare
3	ePXA	5	Geographic, small focus	Not present	Present; rare
4	ePXA	5	Pseudopalisading and geographic, small foci	Present	Present
5	ePXA	7	Pseudopalisading and geographic	Present	Present
6	eGBM	30	Geographic, extensive	Present	Absent
7	eGBM	7	Pseudopalisading and geographic	Present	Absent
8	eGBM	15	Pseudopalisading and geographic, extensive	Present	Absent
9	eGBM	12	Geographic and focally pseudopalisading	Present	Absent
10	eGBM	5	Geographic	Present	Absent
11	eGBM	16	Geographic; a small focus of pseudopalisading	Present	Absent
12	eGBM	30	Pseudopalisading; geographic occasionally	Present	Absent
13	eGBM	7	Geographic	Absent	Absent
14	eGBM	15	Pseudopalisading	Present	Absent
15	eGBM	8	Absent	Present, rare foci	Absent
16	eGBM	4	Pseudopalisading	Present	Absent

**Table 3.** Summary of the immunohistochemical stains. Abbreviations: ND = not done; ePXA = epithelioid pleomorphic xanthoastrocytoma; eGBM = epithelioid glioblastoma.

Case No.	Diagnosis	Reticulin	GFAP	Olig2	NF	Synaptophysin	CD34	EMA	Ki67	Vimentin
1	ePXA	Rich in PXA/poor in epithelioid	Focal in PXA/negative in epithelioid	Positive in PXA/negative in epithelioid	Mostly solid; occasional tumor cells	Weak; occasional epithelioid cells positive	Patchy; arborescent pattern	Patchy	3% in PXA; 90% in epithelioid	Extensive
2	ePXA	Poor	Focal	Focal in PXA	Mostly solid; rare tumor cells	Focal in tumor cells	Negative	Patchy	8% in PXA; 30% in epithelioid	Extensive
3	ePXA	Rich in PXA areas/poor in epithelioid	Occasional	Negative	Mostly solid; negative in tumor cells	Negative	Negative	Patchy	10% in epithelioid; not done in PXA	Extensive
4	ePXA	Rich in PXA/poor in epithelioid	Extensive	ND	Mostly solid; negative in tumor cells	Occasional cells	Positive; arborescent pattern	Patchy	2.5% in PXA; 11.8% in epithelioid	Extensive
5	ePXA	Rich in PXA/poor in eGBM	Positive in PXA/negative in eGBM	Patchy; more in PXA	Mostly solid; rare tumor cells	Occasional tumor cells	Focal; arborescent pattern	Patchy	12% in PXA; 50% in epithelioid	Extensive
6	eGBM	ND	Patchy	Focal	ND	Negative	Negative	Patchy	50%	ND
7	eGBM	ND	Negative	Negative	Mostly solid; negative in tumor cells	ND	Negative	Patchy	ND	Extensive
8	eGBM	ND	Focal	Negative	Mostly solid; occasional tumor cells	Focal in tumor cells	Rare; membrane staining	Patchy	ND	Extensive
9	eGBM	ND	Occasional	Negative	Mostly solid; occasional tumor cells	Rare tumor cells	Negative	Negative	ND	Extensive
10	eGBM	ND	Rare cells	Negative	Mostly solid; negative in tumor cells	Positive in a subset of tumor cells	Negative	Patchy	ND	Extensive
11	eGBM	ND	Focal	ND	Infiltrative; negative in tumor cells	Negative	Focal; membrane staining	Rare tumor cells	ND	ND
12	eGBM	ND	Extensive	ND	Mostly solid; occasional tumor cells	Negative	Negative	Patchy	ND	ND
13	eGBM	ND	Focal	ND	Mostly solid; negative in tumor cells	Negative	Negative	Negative	ND	ND
14	eGBM	ND	Extensive	ND	Mostly solid; negative in tumor cells	Negative	Rare; membrane staining	Rare tumor cells	ND	ND
15	eGBM	ND	Focal; less in epithelial areas	Extensive	Infiltrative; occasional tumor cells	Occasional tumor cells	Extensive; membrane staining	Negative	17%	Extensive
16	eGBM	ND	Negative	Rare cells	Infiltrative; negative in tumor cells	Occasional entrapped neurons	ND	Patchy	ND	ND

**Table 4.** Molecular characteristics of the cases of ePXA and eGBM. Abbreviations: ND = not done; NI = not interpretable.

Case No.	p53 (IHC)	IDH1 (R132H) (IHC)	ATRX (IHC)	INI1(BAF47) (IHC)	BRG1 (IHC)	<i>BRAF V600E</i> (IHC)	EGFR amplification (FISH)	PTEN deletion (FISH)	ODZ3 deletion (FISH)	H3 K27M (IHC)
1	Negative	ND	ND	Retained	Retained	Positive	ND	ND	Negative	ND
2	Positive	ND	ND	Retained	Retained	Negative	Negative	Negative	Negative	ND
3	Negative	ND	ND	Retained	Retained	Positive	ND	ND	Deletion	ND
4	Negative	ND	ND	ND	ND	Positive	ND	ND	Negative	ND
5	Positive	ND	ND	Retained	ND	Positive	Negative	Negative	Deletion	ND
6	Positive	Negative	Retained	Retained	Retained	Negative	Negative	ND	Deletion	Negative
7	Positive	Negative	Retained	Retained	Retained	Positive	Negative	Monosomy 10	Negative	Negative
8	Negative	Negative	Retained	Retained	Retained	Positive	Negative	ND	Deletion	Negative
9	Negative	Negative	Retained	Retained	Retained	Negative	Negative	Deletion	Deletion	ND
10	Positive	Negative	Retained	Retained	ND	Negative	Negative	ND	Deletion	ND
11	Negative	Negative	ND	Retained	ND	Negative	Negative	ND	Deletion	Negative
12	Negative	Negative	ND	Retained	ND	Positive	Negative	Negative	Deletion	Negative
13	Negative	Negative	ND	Retained	ND	Positive	Negative	Negative	ND	Negative
14	Negative	Negative	ND	Retained	ND	Negative	Negative	Negative	Deletion	Negative
15	Positive	Negative	Lost	Retained	ND	Negative	Negative	Negative	Negative	Positive
16	ND	Negative	ND	ND	ND	ND	Negative	ND	NI	ND

(40%) and four eGBMs (40%). The *BRAF*<sup>V600E</sup> immunostain was positive in both components of 4 ePXAs (80%) and in 4 of the 10 eGBMs in which it was performed (40%) (Figure 3G,H). The Ki-67 labeling index was low in the PXA areas of ePXA (Figure 3I) and high in the epithelioid areas of all cases in which it was performed (Figure 3J). Case 15 was unique in the series in that it was the only case with H3 K27M mutant protein expression and loss of ATRX. It additionally had a small focus resembling ganglioglioma, which similarly expressed H3 K27M, but retained nuclear ATRX expression.

### Fluorescence *in situ* hybridization

FISH for *ODZ3* gene could not be performed on one consult case due to lack of additional unstained slides and paraffin blocks. Furthermore, in one case, the signals could not be accurately interpreted. Seven of the remaining nine eGBM cases (77.8%) and two of the ePXA cases (40%) demonstrated hemizygous deletion

of *ODZ3* gene at 4q34.3–4q35.1 (Figure 4). Of these eGBMs, three were pediatric and four were adult. The ePXAs with deletion were both pediatric. Both eGBMs and ePXAs in this study were composed in great part of areas with epithelioid morphologic features and the majority of cells in which the FISH signals were counted were therefore epithelioid.

Five eGBMs (45.5%) showed polysomy 7 (3–5 centromeres and EGFR signals per cell), but none had evidence of EGFR gene amplification. Monosomy of chromosome 10 was present in a pediatric case of eGBM and more localized PTEN (10q) deletion was found in one adult case of eGBM.

### Methylome signatures

The adult ePXA (case 2) had a methylation pattern that clustered with that of other histologically classic PXAs studied in Heidelberg, Germany (not part of current study) (10). One pediatric eGBM with *ODZ3* gene deletion (case 12) similarly had

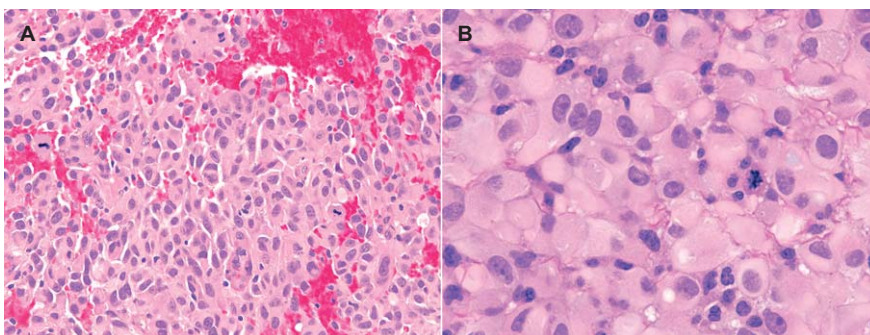


**Figure 2.** **A.** Hematoxylin–eosin-stained (H&E) section of an epithelioid area in a case of ePXA (case 5), demonstrating sheets of loosely cohesive cells with abundant eosinophilic cytoplasm, large, occasionally eccentric nuclei, occasional nucleoli and distinct cellular borders (melanoma-like features). A high mitotic rate is observed. **B.** A high-power microscopic field of an eGBM (case 6), demonstrating epithelioid cells with the same features as described above. Occasional cells with paranuclear globular inclusions are seen (rhabdoid features); furthermore, there are occasional cells with enlarged red macronucleoli (melanoma-like features).

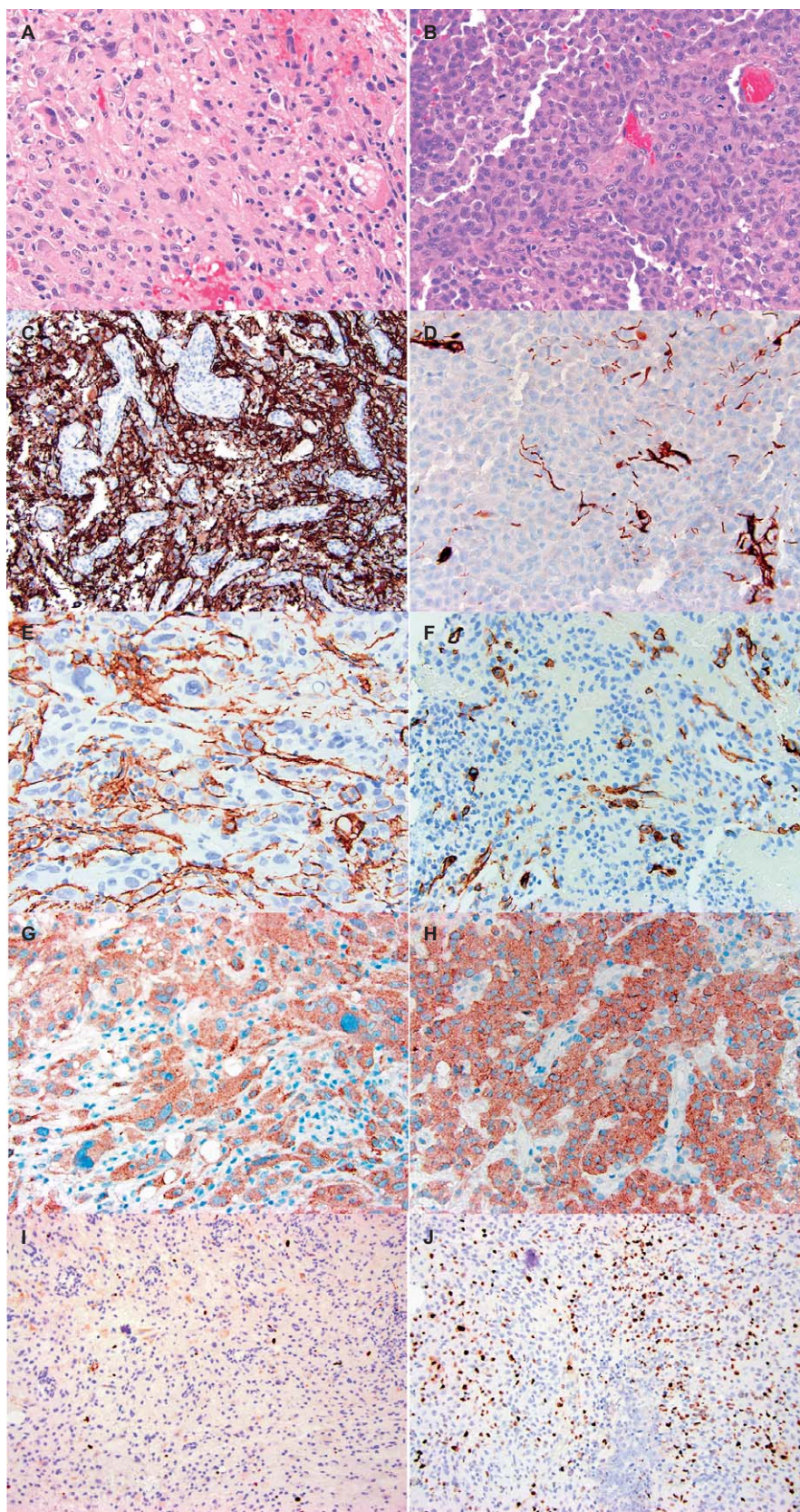


**Figure 3.** Comparison of morphologic and immunohistochemical features of PXA (left) and epithelioid (right) areas in a single case of ePXA (case 5). **A.** Illustrates an area composed of spindled and oval cells with irregular nuclear contours and variably vacuolated (lipidized) cytoplasm. Eosinophilic granular bodies and occasional bizarre, large cells are also seen. **B.** Shows the epithelioid regions of anaplastic transformation. The PXA areas were extensively positive for GFAP (cytoplasmic and fibrillary pattern) (**C**), whereas the epithelioid areas showed mostly loss of GFAP expression (**D**). Occasional tumor cells in the PXA areas demonstrated CD34 expression in an arborescent pattern (**E**). The epithelioid areas also contained occasional CD34-positive tumor cells (**F**). Both areas demonstrated *BRAF V600E* mutant protein expression (**G,H**). The Ki67 immunostain revealed a low proliferation index in the PXA areas (**I**), and a considerably higher labeling index in the epithelioid areas (**J**).

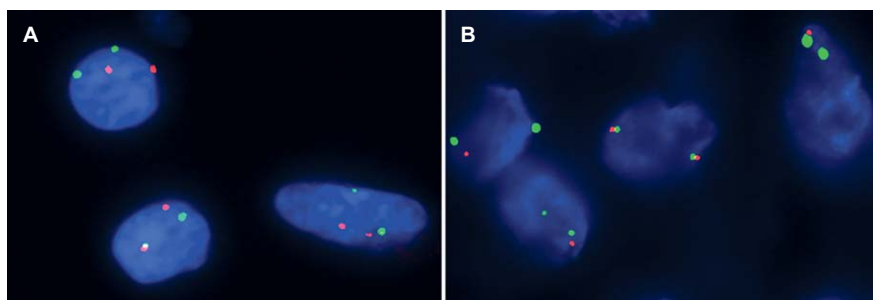


**Figure 4.** **A.** Illustrates a non-neoplastic control case with two CEP4 signals (green) and two ODZ3 signals (red) in most nuclei. **B.** Illustrates a case of eGBM in which the majority of nuclei contain one ODZ3 (red) and two CEP4 (green) signals.

a methylation pattern that clustered with the PXAs and another pediatric GBM (case 13) had a methylation pattern that clustered with the low-grade astrocytomas. The remaining two cases of eGBM clustered with histologically classic examples of pediatric GBM studied in Heidelberg, Germany (not part of current study). The results of Illumina Human Methylation450 BeadChip (450k) array for the five cases are summarized in Table 5.

**DISCUSSION**

eGBM is a very rare variant of GBM that is not included in the 2007 WHO classification scheme (14). Only case reports and a few small series have been previously reported (2, 8). It is usually seen within the first three decades of life and the majority of cases are primary (ie, no previously established lower grade precursor). The course of eGBM is an aggressive one and is often complicated by early recurrence, intratumoral hemorrhage and leptomeningeal spread (2). Nevertheless, surprisingly long survival times have been reported in a subset (1, 8) as was found also in a subset of our own patients. Additionally, dramatic responses to BRAF inhibitors have been reported anecdotally in V600E mutant examples, emphasizing that this variant may have several important differences from that of conventional GBM (4, 12, 21). Most of the time, this variant also differs in that it does not show *EGFR* amplification, *IDH1* gene mutation or *PTEN* deletion, but instead, about half of these cases harbor *BRAF V600E* mutation (8), a finding that remained true in our study as well.

eGBM is difficult to distinguish from PXA with anaplastic transformation with epithelioid features (ePXA), another subtype that is not described in the 2007 WHO scheme, but has been reported rarely (6). In our series, ePXA behaved clinically similar to

the eGBMs, with recurrences within months of initial resection, and leptomeningeal dissemination, although in both tumor types, some long survival times were also seen. In the current study, we found no reliable demographic, radiologic, histologic, immunohistochemical or molecular differences between the two glioma subtypes, with the only distinction being definitional, in that a classic area of low-grade PXA is found in ePXA but not in eGBM. This raises the possibility that at least in some eGBM, a precursor PXA component may be overrun by the more malignant epithelioid component or was not sampled in the resection specimen. Supporting this hypothesis is the fact that in one of our cases, the PXA component accounted for no more than 5% of the entire tumor and was relatively inconspicuous in comparison to the adjacent, more abundant epithelioid elements. Furthermore, methylome analysis showed that one of our four tested eGBMs had a methylation pattern that clustered with conventional PXA. Lastly, a case recently reported by Tanaka *et al* (26) showed an eGBM developing within the tumor bed of a PXA 13 years after initial resection. All these data suggest that eGBM and ePXA are either the same entity or highly related.

Nevertheless, one of our eGBM cases was associated with the H3 K27M molecular subtype of high-grade glioma and one of the eGBM cases previously reported by Kleinschmidt-DeMasters *et al* was IDH mutant (8). As such, it is possible that the epithelioid phenotype can also represent a secondary pattern in other more classically described molecular subtypes of GBM. Therefore, there remain a number of unanswered questions regarding WHO nomenclature (PXA vs. GBM), grade (III vs. IV), and whether such cases should be considered part of a unique entity, a distinct variant, or merely a morphologic pattern that can be encountered in more than one molecularly defined GBM subtype.

**Table 5.** Results of the genome-wide methylation studies performed on five of the cases (10). Abbreviations: LGA = low-grade glioma; Mut. = mutated; WT = wild type; PXA = pleomorphic xanthoastrocytoma; GBM = glioblastoma.

Case No.	450k array clustering pattern	H3F3A	IDH1 (R132H)	BRAF V600E	Amplifications	Homozygous deletions	Gains	Losses
2	PXA	WT	WT	WT	None	CDKN2A	5, 7, 9q, 12p, 14q, 16q, 22q	1, 6, 13q, 14q, 21q
11	GBM	WT	WT	WT	None	None	7	1p, 3p, 6, 8, 9p, 10p, 13q, 14q, 17p, 22q
12	PXA	WT	WT	Mut.	None	None	None	None
13	LGA	WT	WT	Mut.	None	None	None	None
14	GBM	WT	WT	WT	None	None	None	None

## ACKNOWLEDGMENTS

We thank Roxanne Marshall for her help and expertise in setting up and performing fluorescence *in situ* hybridization. The authors have no conflict of interest to declare.

## REFERENCES

- Babu R, Hatef J, McLendon RE, Cummings TJ, Sampson JH, Friedman AH, Adamson C (2013) Clinicopathological characteristics and treatment of rhabdoid glioblastoma. *J Neurosurg* **119**:412–419.
- Broniscer A, Tatevossian RG, Sabin ND, Klimo P Jr, Dalton J, Lee R *et al* (2014) Clinical, radiological, histological and molecular characteristics of paediatric epithelioid glioblastoma. *Neuropathol Appl Neurobiol* **40**:327–336.
- Chakrabarty A, Mitchell P, Bridges LR, Franks AJ (1999) Malignant transformation in pleomorphic xanthoastrocytoma—a report of two cases. *Br J Neurosurg* **13**:516–519.
- Chamberlain MC (2013) Salvage therapy with BRAF inhibitors for recurrent pleomorphic xanthoastrocytoma: a retrospective case series. *J Neurooncol* **114**:237–240.
- Dias-Santagata D, Lam Q, Vernovsky K, Vena N, Lennerz JK, Borger DR *et al* (2011) BRAF V600E mutations are common in pleomorphic xanthoastrocytoma: diagnostic and therapeutic implications. *PLoS ONE* **6**:e17948.
- Iwaki T, Fukui M, Kondo A, Matsushima T, Takeshita I (1987) Epithelial properties of pleomorphic xanthoastrocytomas determined in ultrastructural and immunohistochemical studies. *Acta Neuropathol* **74**:142–150.
- Kepes JJ (1993) Pleomorphic xanthoastrocytoma: the birth of a diagnosis and a concept. *Brain Pathol* **3**:269–274.
- Kleinschmidt-Demasters BK, Aisner DL, Birks DK, Foreman NK (2013) Epithelioid GBMs show a high percentage of BRAF V600E mutation. *Am J Surg Pathol* **37**:685–698.
- Kleinschmidt-DeMasters BK, Alassiri AH, Birks DK, Newell KL, Moore W, Lillehei KO (2010) Epithelioid versus rhabdoid glioblastomas are distinguished by monosomy 22 and immunohistochemical expression of INI-1 but not claudin 6. *Am J Surg Pathol* **34**:341–354.
- Korshunov A, Ryzhova M, Hovestadt V, Bender S, Sturm D, Capper D *et al* (2015) Integrated analysis of pediatric glioblastoma reveals a subset of biologically favorable tumors with associated molecular prognostic markers. *Acta Neuropathol* **129**:669–678.
- Lath R, Unosson D, Blumbergs P, Stahl J, Brophy BP (2003) Rhabdoid glioblastoma: a case report. *J Clin Neurosci* **10**:325–328.
- Lee EQ, Ruland S, LeBoeuf NR, Wen PY, Santagata S (2014) Successful treatment of a progressive BRAF V600E-mutated anaplastic pleomorphic xanthoastrocytoma with vemurafenib monotherapy. *J Clin Oncol* **32**. doi: 10.1200/JCO.2013.51.1766.
- Letouze E, Rosati R, Komechen H, Doghman M, Marisa L, Fluck C *et al* (2012) SNP array profiling of childhood adrenocortical tumors reveals distinct pathways of tumorigenesis and highlights candidate driver genes. *J Clin Endocrinol Metab* **97**:E1284–E1293.
- Louis DN, Ohgaki H, Wiestler OD, Cavenee WK (2007) *WHO Classification of Tumours of the Central Nervous System*, 4th edn. IARC: Lyon.
- Marton E, Feletti A, Orvieto E, Longatti P (2007) Malignant progression in pleomorphic xanthoastrocytoma: personal experience and review of the literature. *J Neurol Sci* **252**:144–153.
- Molenaar JJ, Koster J, Zwijnenburg DA, van Sluis P, Valentijn LJ, van der Ploeg I *et al* (2012) Sequencing of neuroblastoma identifies chromothripsis and defects in neuritogenesis genes. *Nature* **483**:589–593.
- Momota H, Iwami K, Fujii M, Motomura K, Natsume A, Ogino J *et al* (2011) Rhabdoid glioblastoma in a child: case report and literature review. *Brain Tumor Pathol* **28**:65–70.
- Nagayama K, Kohno T, Sato M, Arai Y, Minna JD, Yokota J (2007) Homozygous deletion scanning of the lung cancer genome at a 100-kb resolution. *Genes Chromosomes Cancer* **46**:1000–1010.
- Nobusawa S, Hirato J, Kurihara H, Ogawa A, Okura N, Nagaishi M *et al* (2014) Intratumoral heterogeneity of genomic imbalance in a case of epithelioid glioblastoma with BRAF V600E mutation. *Brain Pathol* **24**:239–246.
- Reis GF, Pekmezci M, Hansen HM, Rice T, Marshall RE, Molinaro AM *et al* (2015) CDKN2A loss is associated with shortened overall survival in lower-grade (World Health Organization Grades II–III) astrocytomas. *J Neuropathol Exp Neurol* **74**:442–452.
- Robinson GW, Orr BA, Gajjar A (2014) Complete clinical regression of a BRAF V600E-mutant pediatric glioblastoma multiforme after BRAF inhibitor therapy. *BMC Cancer* **14**:258.
- Rodriguez FJ, Scheithauer BW, Giannini C, Bryant SC, Jenkins RB (2008) Epithelial and pseudoepithelial differentiation in glioblastoma and gliosarcoma: a comparative morphologic and molecular genetic study. *Cancer* **113**:2779–2789.
- Rosenblum MK, Erlandson RA, Budzilovich GN (1991) The lipid-rich epithelioid glioblastoma. *Am J Surg Pathol* **15**:925–934.
- Sturm D, Witt H, Hovestadt V, Khuong-Quang DA, Jones DT, Konermann C *et al* (2012) Hotspot mutations in H3F3A and IDH1 define distinct epigenetic and biological subgroups of glioblastoma. *Cancer Cell* **22**:425–437.
- Takami H, Yoshida A, Fukushima S, Arita H, Matsushita Y, Nakamura T *et al* (2015) Revisiting TP53 mutations and immunohistochemistry—a comparative study in 157 diffuse gliomas. *Brain Pathol* **25**:256–265.
- Tanaka S, Nakada M, Nobusawa S, Suzuki SO, Sabit H, Miyashita K, Hayashi Y (2014) Epithelioid glioblastoma arising from pleomorphic xanthoastrocytoma with the BRAF V600E mutation. *Brain Tumor Pathol* **31**:172–176.
- Wyatt-Ashmead J, Kleinschmidt-DeMasters BK, Hill DA, Mierau GW, McGavran L, Thompson SJ, Foreman NK (2001) Rhabdoid glioblastoma. *Clin Neuropathol* **20**:248–255.